



A detailed investigation of the corrected BEM method and the potential for improving blade design

Døssing, Mads

Published in:
EWEC 2009 Proceedings online

Publication date:
2009

Document Version
Publisher's PDF, also known as Version of record

[Link back to DTU Orbit](#)

Citation (APA):
Døssing, M. (2009). A detailed investigation of the corrected BEM method and the potential for improving blade design. In *EWEC 2009 Proceedings online* EWEC.

General rights

Copyright and moral rights for the publications made accessible in the public portal are retained by the authors and/or other copyright owners and it is a condition of accessing publications that users recognise and abide by the legal requirements associated with these rights.

- Users may download and print one copy of any publication from the public portal for the purpose of private study or research.
- You may not further distribute the material or use it for any profit-making activity or commercial gain
- You may freely distribute the URL identifying the publication in the public portal

If you believe that this document breaches copyright please contact us providing details, and we will remove access to the work immediately and investigate your claim.

A DETAILED INVESTIGATION OF THE CORRECTED BEM METHOD AND THE POTENTIAL FOR IMPROVING BLADE DESIGN

Mads Døssing

MSc, Mech. Eng. PhD student, Aeroelastic Design
Risø DTU National Laboratory for Sustainable Energy
mads.doessing@risoe.dk

Abstract:

Improved BEM models with corrections for wake rotation and expansion are superior to the standard BEM method in predicting flow properties in the tip and root sections of blades for horizontal axis wind turbines. Turbines optimized for improved aerodynamics using the advanced models are. Special attention is on effects not captured by standard BEM methods and if the design can be improved based on this. The accuracy of the newly developed advanced BEM model is discussed.

Keywords: BEM, BEM corrections, optimization, wake rotation, wake expansion

0 Nomenclature

R	Rotor radius	m
P	Power	W
T	Thrust	N
V_0	Undisturbed wind speed	m/s
v_a	Axial wind speed in rotorplane	m/s
Ω	Rotational speed	s ⁻¹
λ	Tip speed ratio	-
λ_l	Local speed ratio	-
a	Axial induction factor	-
a_{eff}	Effective axial induction	-
a'	Tangential induction factor	-
k_1	$a(C_F/F)$ correlation constants	-
k_2		-
k_3		-
C_P	Power coefficient	-
C_T	Thrust coefficient	-
$C_{F,\%}$	Flapwise moment coefficient About % radial position	-
C_F	Flapwise moment coefficient About rotor centre	-
C_p	Local power coefficient	-
C_t	Local thrust coefficient	-
F	Prandtl's tip loss factor	-

Δv_w	Correction for wake rotation	-
Δv_a	Correction for wake expansion	-
Δv_m	Corr. for unchanged mass flow	-
C_v	Local force coefficient, flap	-
C_x	Local force coefficient, edge	-
l	Local lift force	N
d	Local drag force	N
C_l	Local lift coefficient	-
C_d	Local drag coefficient	-
ρ	Density	kg/m ³
v_t	Local tangential velocity	m/s
v_n	Local normal velocity	m/s
v_{rel}	Local relative velocity	m/s
α	Angle of attack	rad.
φ	Local flowangle	rad.
c	Chord	m
M_F	Flapwise moment	Nm
r	Coordinate, radius	m
r_0	Evaluation radius of M_F	m
Γ	Bound circulation	m ² /s
N_B	Number of blades	-

1 Introduction

The blade element momentum (BEM) method in its original form has in recent years been subjected to a thorough investigation with the purpose of determining its accuracy. Among other issues this has led to the conclusion that the power production from the inner part of the blade is underestimated and conversely overestimated on the outer part. The cause for this is believed to be the failure of the BEM method to accurately predict the axial velocities, for a given loading, correct. For wind turbines in normal operation the rotation of the wake causes an acceleration of the axial flow on the inner part and the wake expansion causes a deceleration on the outer part. Both effects are not captured in the standard BEM model. These issues have been treated in detail in Madsen et al. [1] & [2] and the results are the BEM corrections for the

axial flow. If these are implemented, the method is denoted corrected or improved blade element momentum method (BEM_{cor}).

In Madsen et al. [1] & [2] the main focus is on the derivation of the corrections and the corrected velocities are validated against an actuator disc (ACD) calculation. This is done for a defined loading, thus no iterations are performed. In the following the corrections have been implemented in a full BEM_{cor} algorithm in order to validate the results when the loading is updated according to the velocities in the rotor plane. Notice that the results of BEM_{cor} are sensitive to the order in which various properties are updated when iterating. A full description of the implementation is found in Madsen et al. [1].

The present work is a fundamental study of the importance of the BEM corrections, i.e. how large is the influence from wake rotation and expansion. The best and worst case scenarios are therefore deliberately sought and the blade-designs may deviate from what is reasonable from a manufacturers point of view. E.g. the chord is unconstrained and very large near the blade root, but still sensible at a tip speed ratio of 8. However, an unconstrained optimization is necessary in order to make sure the full potential of the wake rotation is utilized. Blades optimized for maximum power are studied, but also more realistic blades. The latter are defined by optimizing for maximum power to thrust ratio which results in a reasonable low thrust level.

Outline of the article:

- Section 2 gives an introduction to BEM_{cor}, and the optimization algorithm is described.
- In section 3 the BEM_{cor} method is validated.
- Section 4 is a study of unconstrained optimization for maximum power using BEM_{cor} and BEM
- Section 5 is a comparison study of BEM and BEM_{cor} calculations for a series of blades designed using BEM_{cor} and unconstrained optimization of the power to thrust ratio.

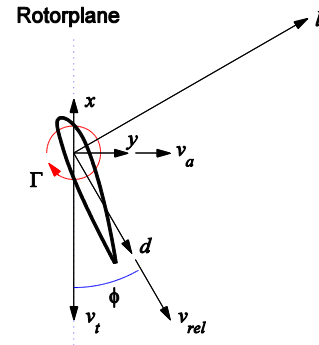


Figure 1 Sketch of the local forces and velocities

2 Method

2.1 The modified BEM method

A full description of the classic BEM method can be found in O.L. Hansen [4] or Glauert [5]. In the following, only the changes introduced in BEM_{cor} is described, which basically applies to a few equations. For a full description, see Aa. Madsen et.al [1].

The corrected BEM model differs from the classic BEM model mainly in the calculation of the axial induction a , which is a measure of the deceleration of the flow in the rotorplane relative to far upstream.

A normal force coefficient C_y is determined by projecting the lift l and drag d (see Figure 1)

$$C_y = \frac{l \cos \varphi + d \sin \varphi}{\frac{1}{2} \rho v_{rel}^2 c}$$

v_{rel} is the relative speed of air, φ is the flowangle relative to the rotorplane, ρ is the density and c is the chord length. In the classic BEM model the axial induction is then determined

$$a = \frac{1}{\frac{8\pi r F \sin^2 \varphi}{C_y c N_B} + 1} \quad (1)$$

Where F is Prandtl's tip loss factor, r is the radius and N_B is the number of blades. The axial velocity v_a in the rotorplane is

$$\frac{v_a}{V_0} = 1 - a \quad (2)$$

Where V_0 is the undisturbed wind speed. Equation (1) is only valid if a is smaller than approx. $a < 0.3$. If $a > 0.3$ an empirical relation must be used.

In BEM_{cor} equations (1) and (2) are replaced. First, instead of (1) the following correlation formula is used

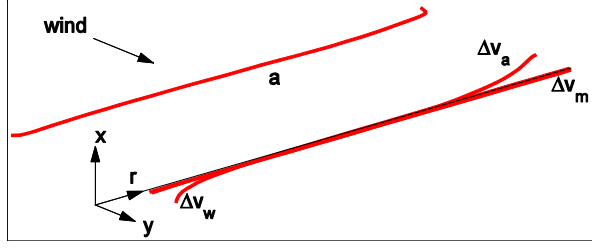


Figure 2 Illustration of the axial induction and corrections along a blade rotating about the y-axis. $C_P=0.505$

$$a = k_3 \left(\frac{C_t}{F} \right)^3 + k_2 \left(\frac{C_t}{F} \right)^2 + k_1 \frac{C_t}{F} \quad (3)$$

Where the local thrust C_t is defined as

$$C_t = \frac{v_{rel}^2 C_x c N_B}{V_0^2 2\pi r} \quad (4)$$

In the case of an *undeflected uncone*d rotor, the constants are

$$k_3 = 0.08921, k_2 = 0.05450, k_1 = 0.25116$$

Notice that (3) is valid for a heavily loaded rotor, i.e. $a > 0.3$.

Equation (2) is now replaced by the following

$$\frac{v_a}{V_0} = 1 - (a - \Delta v_w + \Delta v_a - \Delta v_m) \quad (5)$$

Where Δv_w , Δv_a and Δv_m are the corrections for wake rotation, wake expansion and unchanged mass flow, respectively. An effective axial induction a_{eff} can now be defined

$$a_{eff} = a - \Delta v_w + \Delta v_a - \Delta v_m \quad (6)$$

Figure 2 illustrates the order of magnitude of the terms in a_{eff} for a turbine at $C_P=0.505$.

2.2 Optimization algorithm

The optimization algorithm is an unconstrained steepest descent method with steplength determined by the golden section method. See e.g. Sun and Yuan [9]. The design variables are 36 discrete values of a_{eff} distributed over the blade using a cosine spacing to pack the blade elements closer near the root and tip. Since a_{eff} is a design variable the chord is varied in order to change the axial forces accordingly. In each BEM_{cor} iteration a is determined using (6), then C_t is determined using (3) and finally c is found from (4). All other properties are updated according to the normal BEM_{cor} algorithm as described in Aa. Madsen et.al [1]. The twist is defined to be the inflow angle corrected by the design angle of attack.

The optimization objective is either the power

$$obj = -C_P \quad (7)$$

Or the power to thrust ratio

$$obj = -\frac{C_P}{C_T} \exp \left[\frac{-\left(C_P - C_{P,design} \right)^2}{2 \cdot 0.05^2} \right] \quad (8)$$

In the latter case the exponential is a penalty function included to keep C_P close to the desired value $C_{P,design}$.

3 Validation of BEM_{cor}

The corrected BEM is validated against the optimum rotor presented in Johansen et.al [3], for which actuator disc data is available. The design data for the turbine is summarized in Table 1.

R	63.0 m
N_B	3
2D profile	Risoe B1-15 (15% thickness)
$\lambda = \Omega R / V_0$	8
Design C_t	1.4
Design α	8.0 degree
Design l/d	110

Table 1 Summary of parameters for optimum C_P rotor in Johansen et al. [3]

The local power coefficient is defined as

$$C_P = \frac{\Omega v_{rel}^2 C_x c N_B}{V_0^3 2\pi} \quad (9)$$

Where C_x is the local edgewise force coefficient

$$C_x = \frac{l \sin \phi - d \cos \phi}{\frac{1}{2} \rho v_{rel}^2 c}$$

Figure 3 shows C_P calculated using BEM, BEM_{cor} and ACD respectively. BEM_{cor} correlates well with the ACD results over most of the blade. Figure 4 shows the local thrust coefficient C_t . Again, the results from BEM_{cor} are closer to the ACD which is especially important on the inner part of the blade.

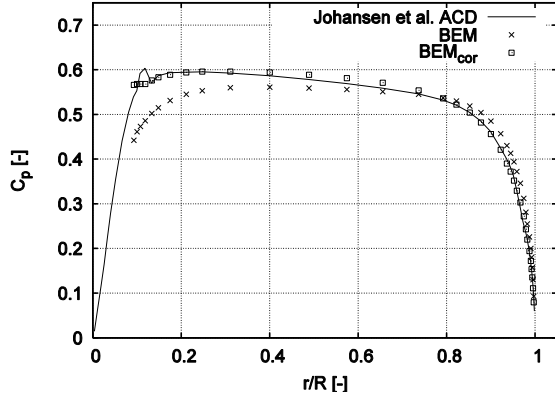


Figure 3 Local power coefficient for optimum rotor

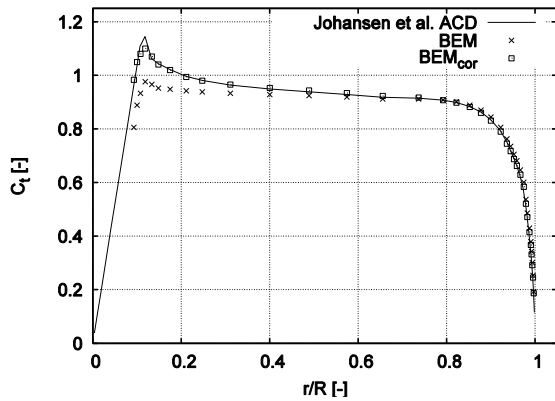


Figure 4 Local thrust coefficient for optimum rotor

Notice that BEM methods cannot converge for very small radii and therefore will integrated results differ slightly from the ACD results. More important is the distribution which correlates well with BEM_{cor}.

Table 2 summarizes the global power and thrust coefficients calculated using various methods. The power and thrust coefficients are defined in the usual way

$$C_P = \frac{P}{\frac{1}{2}\rho V_0^3 \pi R^2}, \quad C_T = \frac{T}{\frac{1}{2}\rho V_0^2 \pi R^2} \quad (10)$$

Where P is the power and T the thrust. BEM_{cor} predicts larger values of C_P and C_T than BEM, and these values are closer to the results reported in Johansen et al. [3] which are based on accurate methods (i.e. ACD and CFD).

Method		C_P	C_T
BEM		0.505	0.858
BEM _{cor}		0.510	0.865
Ellipsys3D (CFD)	Johansen et al. [3]	0.515	0.872
Lifting Line	Johansen et al. [3]	0.514	0.868
Actuator Disc	Johansen et al. [3]	0.510	0.870

Table 2 Performance of optimum rotor

4 Design for optimum C_P

The maximum C_P , which can be obtained using BEM_{cor} has been determined for λ -values from 2 to 12 using the optimization algorithm described earlier. The optimization is unconstrained and large chords are therefore allowed as well as the use of thin profiles on the inner part of the blade. Such a design is not feasible from a manufacturer's point of view but has been selected in order to obtain maximum power. Table 3 summarizes the design parameters.

R	1.0 m
N_B	3
c	Unconstrained
2D profile	Risoe B1-15 (15% thickness)
λ	2,... 12
Design C_l	1.4
Design α	8.0 degree
Design l/d	∞ or 110.0

Table 3 Design parameters for optimization for maximum C_P

Figure 5 shows the results, without tip loss and drag, compared to the results presented by de Vries [8]. The curve representing BEM_{cor} is close to the results by Glauert. This result must be seen in the light of the discussion in de Vries [8] and will not be treated further here.

Figure 6 compares results for BEM and BEM_{cor} if tip loss is included, and both with and without drag. In the former case a constant lift to drag ratio of 110 is defined along the blade. With drag included there is a well defined optimum at $\lambda=8$. Notice that BEM_{cor} shows values which are approx. 1% higher than BEM, thus it is possible to obtain a higher power if BEM_{cor} is used.

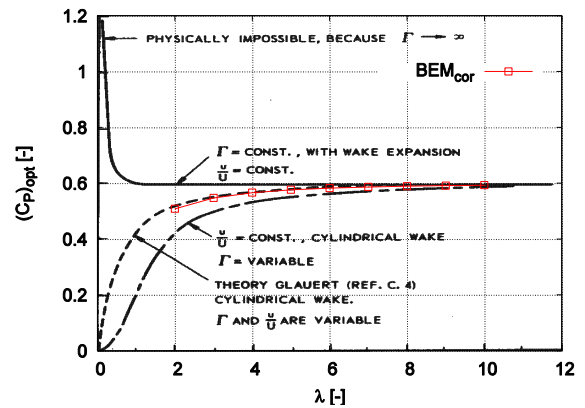


Figure 5 Optimum C_P values using various models for inviscid flow without tip loss. Data is reproduced from de Vries [8]

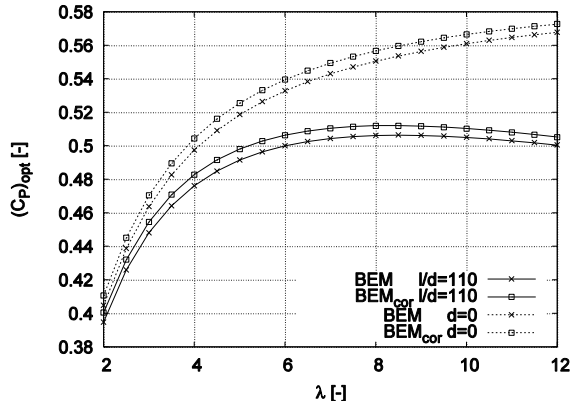


Figure 6 Optimum C_P values using BEM and BEM_{cor} respectively. With tiploss and with and without drag

5 Design for optimum C_P/C_T

In this section the differences between BEM and BEM_{cor} are treated. First, in order to take maximum advantage of the effect of wake rotation, a series of turbines are designed using BEM_{cor} . The design objective is maximum C_P/C_T ratio for 12 values of C_P from $C_P=0.450$ to 0.505 . Table 4 summarizes the design parameters. A tip speed ratio of 8 has been selected and drag is included. Figure 1 shows the optimized chord distributions for $C_P=0.450$, 0.475 and 0.505 .

N_B	3
R	1.0 m
c	unconstrained
2D profile	Risoe B1-15 (15% thickness)
λ	8
Design C_l	1.4
Design α	8.0 degree
Design l/d	110.0

Table 4 Design parameters for optimization for maximum C_P/C_T

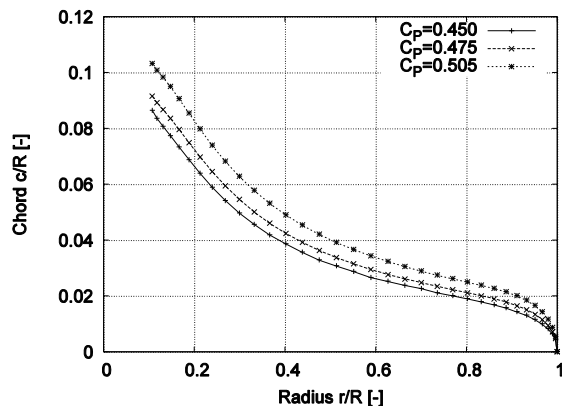


Figure 7 Optimized chord distributions for 3 values of C_P

For the 12 obtained designs the power, thrust and root flap moment is now calculated using BEM and BEM_{cor} respectively. The root flap moment is considered important because of the differences in the distribution of forces predicted by BEM and BEM_{cor} . The results are given in terms of a dimensionless flap coefficient C_F defined in appendix A.

Figure 8 illustrates the difference in performance predicted by BEM and BEM_{cor} . Values of C_T and C_F are plotted against C_P for the 12 turbines. The curves showing BEM results are shifted to the left, i.e. the C_P values are smaller than if calculated using BEM_{cor} . This error in the BEM calculation is approx -0.8%. The exact errors are shown in Table 5, where the errors on C_T and C_F are also stated. The results are given in percentage error of the BEM-value relative to BEM_{cor} . The maximum errors are found for the turbine with the highest loading where the C_P - error is -0.9% and the C_T -error is -0.7%. The errors for less loaded turbines are smaller but still significant. The error on the flap moment is in all cases small, i.e. -0.1%.

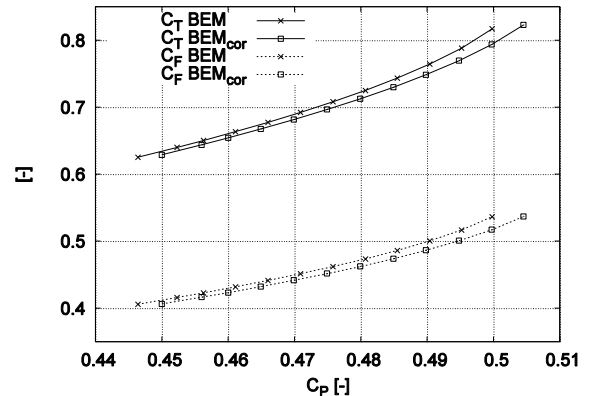


Figure 8 Turbine results calculated using BEM and BEM_{cor}

BEM_{cor}	BEM		
C_P [-]	ΔC_P [%]	ΔC_T [%]	ΔC_F [%]
0.450	-0.80	-0.59	-0.12
0.456	-0.81	-0.61	-0.13
0.460	-0.80	-0.60	-0.12
0.465	-0.82	-0.61	-0.12
0.470	-0.83	-0.63	-0.12
0.475	-0.84	-0.65	-0.12
0.480	-0.85	-0.63	-0.12
0.485	-0.87	-0.66	-0.12
0.490	-0.88	-0.67	-0.12
0.495	-0.89	-0.66	-0.12
0.500	-0.90	-0.69	-0.12

0.505	-0.93	-0.70	-0.12
-------	-------	-------	-------

Table 5 Power, thrust and flap coefficients predicted by BEM, relative to BEM_{cor} values

5.1 Decomposition of C_P

In order to study how the various velocity components and the viscous drag influences the power, C_P is decomposed into 4 contributions from axial velocities and 1 contribution from the drag.

The following dimensionless values are defined

$$\lambda_l = \frac{\Omega r}{V_0}, \quad v_{rel}^* = \frac{v_{rel}}{V_0}, \quad v_a^* = \frac{v_a}{V_0}, \quad v_t^* = \frac{v_t}{V_0}$$

Where the tangential velocity v_t is found from the tangential induction factor a'

$$v_t^* = \lambda_l (1 + a')$$

The relative velocity v_{rel} and the flowangle φ are

$$v_{rel}^* = \sqrt{v_t^{*2} + v_a^{*2}}$$

$$\tan \varphi = \frac{v_a^*}{v_t^*}$$

The contribution to power due to lift forces is by direct integration

$$P(v_a) = N_B \Omega \int_{blade} r^{1/2} \rho v_{rel}^2 c C_l \sin \varphi dr \quad (11)$$

If inviscous flow is assumed the bound circulation Γ is related to the lift

$$\Gamma = 1/2 C_l v_{rel} c$$

(11) can therefore be written as

$$P(v_a) = N_B \Omega \int_{blade} r \rho v_a \Gamma dr$$

Rewriting to dimensionless quantities yields

$$C_P(v_a^*) = \frac{2N_B \lambda}{\pi} \int_{blade} r^* v_a^* \Gamma^* dr^* \quad (12)$$

The definition of the dimensionless bound circulation Γ^* follows directly from the derivation of (12) by collecting the remaining dimensional quantities

$$\Gamma^* = \frac{\Gamma}{V_0 R} \quad (13)$$

Because all other quantities in (12) are constant for fixed tip speed ratio and geometry, it follows that Γ^* must also follow a functional relationship of the form

$$\Gamma^* = f(\lambda)$$

Notice that v_a is also a function of λ . Since (12) is linear it can be split into the following four contributions corresponding to the 4 velocity

components composing v_a^*

$$C_P(1-a) = \frac{2N_B \lambda}{\pi} \int_{blade} r^* \Gamma^* (1-a) dr^* \quad (14)$$

$$C_P(\Delta v_w) = \frac{2N_B \lambda}{\pi} \int_{blade} r^* \Gamma^* \Delta v_w dr^* \quad (15)$$

$$C_P(-\Delta v_a) = \frac{2N_B \lambda}{\pi} \int_{blade} r^* \Gamma^* (-\Delta v_a) dr^* \quad (16)$$

$$C_P(\Delta v_m) = \frac{2N_B \lambda}{\pi} \int_{blade} r^* \Gamma^* \Delta v_m dr^* \quad (17)$$

The power contribution due to drag is

$$P(d) = -N_B \Omega \int_{blade} r^{1/2} \rho v_{rel}^2 c C_d \cos \varphi dr \quad (18)$$

Where the drag coefficient C_d is defined by the lift to drag ratio

$$C_d = \frac{C_l}{C_d} \quad (19)$$

Combining (18) with (19) and rewriting to nondimensional quantities yields

$$C_P(d) = -\frac{2N_B \lambda}{\pi} \int_{blade} r^* v_t^* \Gamma^* dr^* \quad (20)$$

C_P is now decomposed into the contributions from (14), (15), (16), (17) & (20), i.e.

$$C_P = C_P(1-a) + C_P(\Delta v_w) + \dots + C_P(-\Delta v_a) + C_P(\Delta v_m) + C_P(d) \quad (21)$$

In section 5 the blade series was defined by optimization using BEM_{cor}. A decomposition of the obtained C_P -values is seen in Figure 9. The individual BEM corrections contributes with less than (+-)0.2% to the total C_P and the wake expansion correction almost exactly cancels the correction for unchanged mass flow. The contribution from wake rotation is very small. I.e. the optimization-algorithm does not take advantage of the positive effects from wake rotation. The increase in power which can be obtained using BEM_{cor} (see section 4) is therefore not due to any specific flow property introduced by the BEM corrections. It is simply a result of the more accurate method used and the following optimization.

Even though the above results indicates a weak effect due to wake expansion and rotation, this may not be the case on poorly designed turbines. It is also noticed that the correction for unchanged mass flow is important and that it increases the power production on the main part of the blade. This is unfortunate because it is not based on a thorough study.

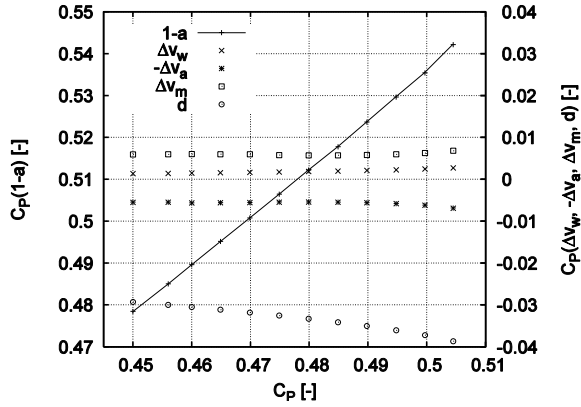


Figure 9 Decomposed components of the C_P -values calculated using BEM_{cor} (in section 5)

7 Conclusion and future work

The implementation of BEM corrections in a BEM algorithm, including the updating of forces, has been validated.

An optimization for maximum power has shown that a C_P of 0.51 can be obtained using BEM_{cor} and a constant lift to drag ratio of 110. If BEM is used the maximum is approx 1% lower, i.e. $C_P = 0.505$.

A comparison of 12 blades has shown that the error using BEM was as high as 0.9% on C_P and 0.7% on C_T , when comparing with BEM_{cor} . The error on the root flap moment was small, approx 0.1%.

The blades were designed using BEM_{cor} . It was found that the optimization algorithm did not take advantage of the positive effects from wake rotation, thus no significant positive effect can be obtained by designing for a strong rotation of the wake.

In future work the presented designs will be compared to results for a real turbine, the NM80.

References

- [1]. Helge Aa. Madsen, Robert Mikkelsen, Christian Bak, Stig Øye, Mads Døssing. *Validation and Modification of the Blade Element Momentum theory based on Comparisons with Actuator Disc Simulations*. Risø DTU. (to be published in 2009).
- [2]. H. Aa. Madsen, R. Mikkelsen, S. Øye, C. Bak, J. Johansen, *A Detailed investigation of the Blade Element Momentum (BEM) model based on analytical and numerical results and*

proposal for modifications of the BEM model. Journal of Physics. 2007.

- [3]. Johansen, J., Aagaard Madsen, H., Gaunaa, M., Bak, C., Sørensen, N.N., *3D Navier-Stokes simulations of a rotor designed for maximum aerodynamic efficiency*. Jan. 2007.
- [4]. Martin O.L. Hansen, *Basic Rotor Aerodynamics applied to Wind Turbines*. ISBN 87-7475-192-1. Technical University of Denmark. 1998.
- [5]. Glauert, H. Airplane Propellers. *Aerodynamic Theory Volume IV*. Edited by William Frederick Durand. The Dover edition 1963.
- [6]. Madsen H.A. *A CFD Analysis of the Actuator Disc Flow compared with Momentum Theory Results* In "proceedings of IEA Joint Action of 10th Symposium on Aerodynamics of Wind Turbines", Edinburg, December 16-17, 1996 edited by B.M. Pedersen, pp. 109-124.
- [7]. Madsen, H. Aa, Rasmussen F. *The influence on energy conversion and induction from large blade deflections*. In: "Wind energy for the next millennium. Proceedings. 1999 European wind energy conference" (EWEC '99), Nice (FR), 1-5 Mar 1999. Petersen, E.L.; Hjulær Jensen, P.; Rave, K.; Helm, P.; Ehmann, H. (eds.), (James and James Science Publishers, London, 1999) p. 138-141
- [8]. de Vries, O. *Fluid Dynamic Aspects of Wind Energy Conversion*. AGARDograph No. 243, Report AGARD-AG-243, NATO Research & Technology Association, Neuilly-sur-Seine, France, 1979.
- [9]. Wenyu Sun and Ya-Xiang Yuan. *Optimization Theory and Methods, Nonlinear Programming*. Springer 2006.

Appendix A. Dimensionless flap moment coefficient

The dimensionless flapwise force on a blade segment is

$$C_y = \frac{l \cos \varphi + d \sin \varphi}{\frac{1}{2} \rho v_{rel}^2 c}$$

Where l and d are 2D lift and drag forces. v_{rel} is the relative speed of air, φ is the flowangle relative to the rotorplane, ρ is the density and c is the chord. r , r_0 and c are non-dimensionalized

$$(r - r_0)^* = \frac{(r - r_0)}{R}, \quad c^* = \frac{c}{R}$$

r_0 is the radius about which the moment is taken (e.g. the blade root). The flapwise moment can be found by direct integration

$$M_F = \int_{blade} C_y \frac{1}{2} \rho v_{rel}^2 c(r - r_0) dr$$

Collecting all nondimensional quantities on the right hand side yields the dimensionless flap moment

$$\frac{M_F}{\frac{1}{2} \rho V_0^2 R^3} = \int_{blade} C_y v_{rel}^{*2} c^* (r - r_0)^* dr^* \quad (22)$$

The flap coefficient is defined as the left hand side multiplied by the number of blades N_B and divided by π

$$C_{F,\%} = \frac{M_F N_B}{\frac{1}{2} \rho V_0^2 R^3 \pi} \quad (23)$$

% refers to the value of r_0/R . If omitted, it is understood that $r_0=0$. Notice that the denominator is the moment from the force on the rotor disc due to the stagnation pressure, had the total force been concentrated at the tip.

For a fixed turbine geometry, all flow quantities on the right hand side of (23) depends on the tip speed ratio only. A functional dependency, equivalent to that of the power and thrust coefficients, therefore holds

$$C_{F,\%} = f(\lambda)$$